Single-Ion Li⁺, Na⁺, and Mg²⁺ Solid Electrolytes Supported by a Mesoporous Anionic Cu-azolate MOF

Sarah S. Park,[†] Yuri Tulchinsky,[†] Mircea Dincă*

Department of Chemistry, Massachusetts Institute of Technology, 77 Massachusetts Avenue, Cambridge, MA 02139, United States

Supporting Information Placeholder

ABSTRACT: A novel Cu(II)-azolate metal-organic framework (MOF) with tubular pores undergoes a reversible single crystal to single crystal transition between neutral and anionic phases upon reaction with stoichiometric amounts of halide or pseudohalide salts. The stoichiometric transformation between the two phases allows loading of record amounts of charge-balancing Li⁺, Na⁺, and Mg²⁺ ions for MOFs. Whereas the halide/pseudohalide anions are bound to the metal centers and thus stationary, the cations move freely within the one-dimensional pores, giving rise to single-ion solid electrolytes. The respective Li⁺, Na⁺, and Mg²⁺-loaded materials exhibit high ionic conductivity values of 4.4 × 10^{-5} S/cm, 1.8×10^{-5} S/cm, 8.8×10^{-7} S/cm. These are the highest values yet observed for MOF solid electrolytes affording single-ion conduction.

Safety concerns, lack of mechanical robustness, and processing difficulties are some of the drivers of current research into solid ion conductors as electrolytes for energy storage devices.^{1,2} An attractive approach to developing new solid electrolytes is the concept of "single-ion" conduction.3 In liquid electrolytes, both anions and cations are mobile, although only the latter require mobility for a functioning battery. The anions need not be mobile, yet their mobility leads to polarization effects, which decrease the operating voltage of the cell. Accumulation of anions at the anode also eventually leads to decomposition of the liquid electrolyte, one of the primary culprits for declining battery performance over time. In single-ion solid conductors, the anions are fixed to the underlying matrix. This prevents anion movement and accumulation and eliminates the polarization effects present in liquid electrolytes.^{3,4} Although most recent research has focused on the development of single-ion conductors for Li-ion batteries, Na- and Mg-ion batteries are expected to benefit from the development of single-ion Na⁺ and Mg²⁺ conductors as well. Here, we show that a new Cu-azolate MOF that allows stoichiometric binding of anions functions as a good conductor for Li+, Na+, and Mg2+ ions. The respective ionic conductivities are the highest for this class materials in the absence of additional anion mobility.

MOFs are excellent platforms for exploring single-ion conductors. They are electrical insulators, are compatible with a wide range of mobile cations, are tunable, and present regular pore networks, which allow, in principle, for swift ion movement. The potential impact of these materials as solid electrolytes has been confirmed by numerous examples of high proton conductivity values reported lately.⁵ Reports of Li⁺, Na⁺, or Mg²⁺ ion conductors are considerably more rare.⁶⁻⁹ This highlights the difficulty of

developing systematic approaches to introduce significant content of free Li⁺, Na⁺, or Mg²⁺ ions in the pores of MOFs.

Several strategies have been effective in this sense. For instance, open metal sites in MOFs may be used to immobilize anions, leaving free, charge-balancing cations in the pores.7 This strategy was successful in the preparation of the first Li⁺ and Mg²⁺ MOF-based solid electrolytes from dihydroxyterephthlate) (Mg-MOF-74). However, because MOFs with open metal sites are often neutral compounds, there is limited driving force for binding anions, and the maximal loading for Li⁺ and Mg²⁺ ions using this strategy has been 1.26 wt% and 2.51 wt%, respectively, not counting cation content pertaining to free electrolyte. An alternative strategy is the post-synthetic functionalization of inorganic secondary building units (SBUs), such as dehydrating and grafting of LiO'Bu in Zr₆O₄(OH)₄(terephthalate)₆ (UiO-66).8 A third approach is the aliovalent substitution of trivalent ions in a MOF SBU by a combination of divalent and monovalent ions, the former replacing the trivalent ion structurally, with the latter remaining mobile. For instance, replacing Sc³⁺ in ScNa(pyrimidine-4,6-dicarboxylate)₂(H₂O)₂ (EHU-1) by combinations of Cd2+ and Li+ or Mn2+ and Na+ affords materials with mobile Li⁺ and Na⁺ ions, respectively. Neither of the last two strategies are quantitative, however. Indeed, grafting and substitution are both substoichiometric, and have led to maximal mobile Li⁺ loadings of 1.06 wt% and 0.08 wt%, respectively, and mobile Na⁺ loadings of 0.26 wt%. The strategy described herein allows for Li⁺, Na⁺, and Mg²⁺ loadings that exceed previous reports, pointing to a potential blueprint for optimizing ion carrier density in solid electrolytes.

Solvothermal reaction between bis(1H-1,2,3-triazolo[4,5b],[4',5'-i])dibenzo-[1,4]dioxin (H₂BTDD) and CuCl₂·2H₂O in an acidic mixture of N,N-dimethylformamide (DMF) and isopropyl alcohol at 65 °C vields emerald-green rod-shaped crystals of ((CH₃)₂NH₂)[Cu₂Cl₃BTDD]·(DMF)₄(H₂O)_{4.5} (MIT-20). X-ray diffraction analysis of a single crystal of MIT-20 revealed a structure consisting of infinite linearly-bridged Cu SBUs with a single crystallographically unique Cu atom. Each Cu²⁺ ion displays a square pyramidal geometry and is coordinated by three independent triazolate ligands, disposed equatorially, and two chlorides, one terminal equatorial, the other bridging to a neighboring Cu atom (Figure 1). Alternate pairs of Cu atoms are connected either by two BTDD²⁻ ligands, or by two BTDD²⁻ ligands and a μ_2 -Cl. The infinite Cu SBUs are connected by BTDD²⁻ linkers and line one-dimensional hexagonal channels with a crystallographic diameter of ~22 Å. The structure of MIT-20 is similar to BTDDbased MOFs reported with Mn, Co, and Ni, and is topologically identical to the MOF-74 series, but differs from these in one critical aspect: whereas the latter are neutral, MIT-20 is formally anionic, with the charge balance provided by dimethylammonium (DMA) cations residing in the pores. Although X-ray analysis revealed significant positional disorder of the DMA cations, ¹H NMR spectroscopy of an acid-digested sample of MIT-20 confirmed their identity and a ratio of nearly 1:1 of DMA:BTDD, in line with our proposed formula (Figure S1).

The free DMA suggested that MIT-20 could function as a host for various cationic species, including Li⁺, Na⁺, or Mg²⁺, and thus provide a platform for developing solid electrolytes in the presence of appropriate solvents. To test this hypothesis, we attempted to remove guest DMF and water molecules from the assynthesized material. Thus, we subjected MIT-20 to a Soxhlet extraction with hot methanol. During this treatment, the initially emerald green crystals gradually turned greenish-yellow (Figure S2), but retained their single-crystal nature. To our surprise, X-ray analysis of one of these resulting crystals revealed that methanol treatment removes one full equivalent of DMAC1 from MIT-20 to provide an overall neutral framework where all remaining halides are bridging. Cu atoms in this neutral phase are octahedral, with a methanol molecule completing the coordination sphere along with three mer-oriented triazolates and two trans-oriented u2-chlorides (Figure S3). Heating a single crystal of the greenish-yellow neutral phase to 100 °C led to a color change to dark red (Figure S2). Single crystal X-ray diffraction analysis revealed that this colour is associated with the loss of the methanol molecule and formation of Cu₂Cl₂BTDD (MIT-20d). MIT-20d exhibits square pyramidal Cu centers with mer-oriented triazolate linkers and trans-\(\mu_2\)-chlorides and is identical to those of M2Cl2BTDD (M = Mn, Co, Ni) (Figure 1).10

Thermogravimetric analysis (TGA) of methanol-exchanged MIT-20 confirmed that methanol loss occurs also in the bulk above 75 °C (Figure S4). Accordingly, bulk samples of MIT-20d were obtained as red microcrystalline powders by heating methanol-exchanged MIT-20 at 100 °C under reduced pressure. The structural changes occurring in moving from anionic MIT-20 to neutral MIT-20d in bulk crystalline samples are evident by powder X-ray diffraction (PXRD) analysis: from the single crystal Xray diffraction analysis, the neutral compound has a larger a parameter, 38.819(4)Å, relative to that of the anionic phase, 37.171(6)Å(Table S3), which leads to a shift of the peaks corresponding to the $(2\overline{1}0)$ and (300) reflections to lower values of 2θ (Figure 2). N₂ adsorption analysis for MIT-20d at 77 K revealed a type IV isotherm, indicative of mesoporosity, with total uptake of ~750 cm³/g (Figure S5). Fits to this isotherm gave a Brunauer-Emmett-Teller (BET) apparent surface area of 2066 m²/g and a pore size distribution peaking at 22.5 Å (Figure S6), in line with the value expected from crystallography (ca. 23 Å) and with the values reported for other M2Cl2BTDD materials.10

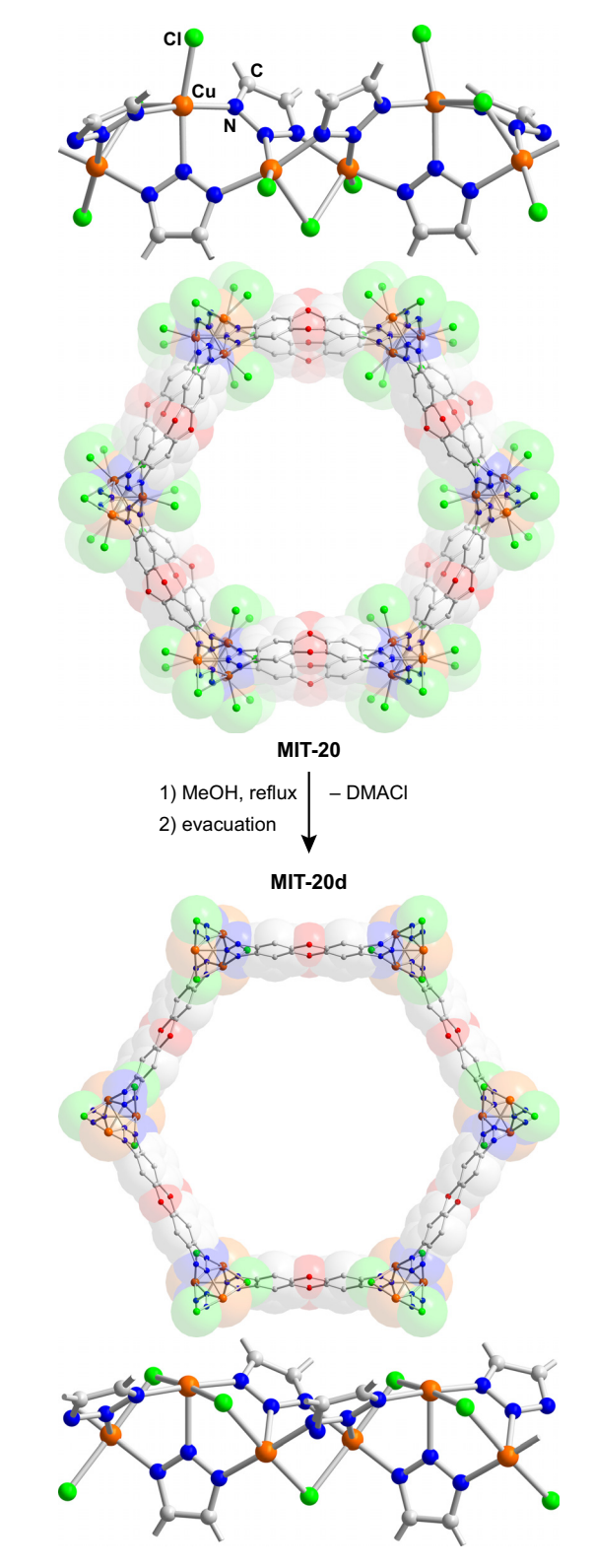


Figure 1. X-ray crystal structures of MIT-20 and MIT-20d, formed from the former by loss of DMACl. The structures of MIT-20-X (X = LiCl, LiBr, Na, Mg), are analogous to MIT-20. H atoms are omitted for clarity.

The preferential formation of MIT-20 under solvothermal conditions suggests that Cu is unique among late first row transition metals in thermodynamically favoring the anionic phase over the neutral one under high chloride concentration. As such, we surmised that treatment of neutral MIT-20d with metal halides

would quantitatively yield anionic phases with a large content of free metal cations residing in the pores. Indeed, treatment of MIT-20d with one equivalent of LiCl in dry tetrahydrofuran (THF) afforded a green microcrystalline powder exhibiting a PXRD pattern identical to that of MIT-20 (Fig. 2, green line). Exchange of residual THF with propylene carbonate (PC), a less volatile solvent with a higher dielectric constant that promotes Li ion conductivity yielded Li[Cu₂Cl₃BTDD]·10(PC) (MIT-20-LiCl) as a free-flowing powder. Inductively-coupled plasma massspectrometry (ICP-MS) analysis of an acid-digested sample of MIT-20-LiCl confirmed a Li:Cu ratio of 1:2. This ratio did not increase even when MIT-20d was treated with excess LiCl, suggesting that the Li content in MIT-20-LiCl, 1.38 wt%, is maximized. Importantly, extensive washing and soaking with dry THF at room temperature did not reduce the Li content of MIT-20-Li, attesting the strong binding of Cl⁻ to the Cu²⁺ ions in this material.

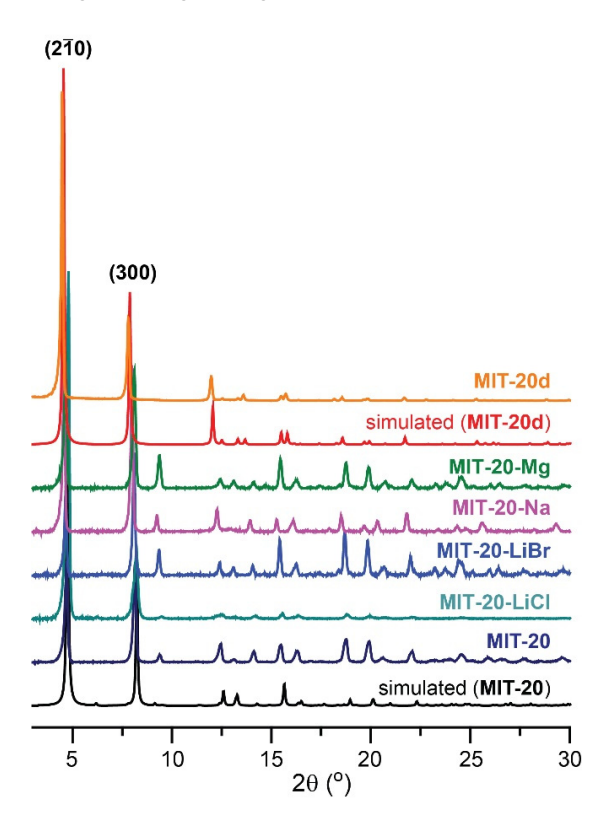


Figure 2. Simulated and experimental PXRD patterns.

The isolation of free cations in the pores of MIT-20 by reacting neutral MIT-20d with metal halides is not limited to Li+. Although NaCl and MgCl2 are nearly insoluble in THF, we were able to access Na⁺ and Mg²⁺-substituted analogs of MIT-20 by reacting MIT-20d with one equivalent of NaSCN or MgBr2 in THF. Upon exchange of residual THF with PC, this led to quantitative formation of Na[Cu₂Cl₂(SCN)BTDD]·9(PC) (MIT-20-Na) and Mg_{0.5}[Cu₂Cl₂BrBTDD]·8(PC) (MIT-20-Mg), respectively, which exhibit record contents of mobile Na⁺ and Mg²⁺ ions of 4.23 wt% and 3.76 wt%, respectively. In all cases, structural retention was verified by PXRD analysis (Figure 2) and the precise content of PC, quantified by ¹H NMR of solutions obtained by digesting the respective MOFs with trifluoroacetic acid (Figure S7), were in line with those observed by TGA (Figure S8). Infrared spectroscopy of MIT-20-Na showed a C-N stretching mode at 2099 cm⁻¹, indicative of metal-bound SCN-, and no residual peaks from free SCN^{-} ($v_{CN} = 2074 \text{ cm}^{-1}$) (Figure S9). This provides additional evidence that all SCN- anions in MIT-20-Na are immobile.

Ionic conductivity measurements for MIT-20-X (X = LiCl, Na, Mg) were performed on powder pellets using alternating current (ac) impedance spectroscopy. Pellets were sandwiched between two stainless steel electrodes under dry N2 in an air-tight cell. Under these conditions, the Nyquist plots obtained for MIT-20-X, shown in Figure 3, exhibit a semi-circle at high frequency and a linear tail at low frequency. The latter is commonly attributed to blocking effects at the electrode and is typical for ionic conductors. 7-9 These plots revealed similar Li⁺ and Na⁺ conductivity values of 1.3×10^{-5} S/cm and 1.8×10^{-5} S/cm for MIT-20-LiCl and MIT-20-Na, respectively, at 25 °C (Table 1). The value for Li⁺ is of the same magnitude as those of Mg₂(dobdc)·0.06LiOⁱPr (σ = 1.2×10^{-5} S/cm)^{7a} and LiO^tBu-grafted UiO-66 ($\sigma = 1.8 \times 10^{-5}$ S/cm),8 whereas the Na⁺ conductivity is highest among single-ion conducting MOFs. The Mg²⁺ ion conductivity in MIT-20-Mg was lower, 8.8×10^{-7} S/cm, as expected for the transport of divalent ions carrying a higher charge density through the otherwise conserved electric field environment of MIT-20. To exclude the contribution of electronic conduction, we measured current-voltage curves for Cu₂Cl₂BTDD(DMF)₂ (Figure S10), which confirmed an electrically insulating behavior, with a conductivity of only 10^{-14} pS/cm in N₂ atmosphere at 25 °C (Figure S11).

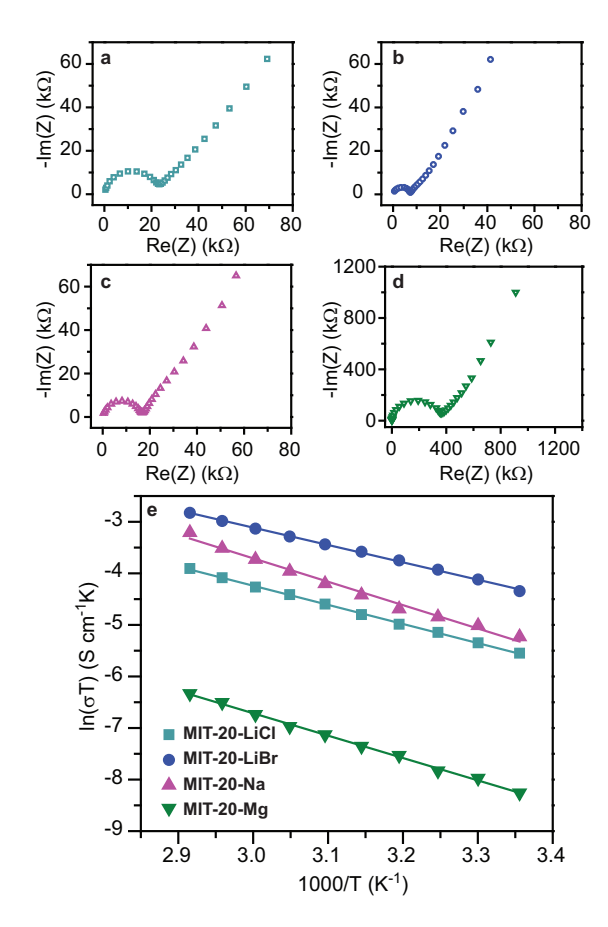


Figure 3. Nyquist plots for (a) MIT-20-LiCl (b) MIT-20-LiBr, (c) MIT-20-Na, and (d) MIT-20-Mg. (e) Ionic conductivities as a function of temperature in the range of 25 °C to 70 °C.

To determine the portion of current carried by lithium ions in MIT-20-LiCl, we conducted lithium transference number measurements using a potentiostatic polarization method. The transference number was $t_{\rm Li^+} = 0.68~(\pm 0.056)$, with certain devices reaching numbers as high as $t_{\rm Li^+} = 0.86$ (Figure S12). These are significantly higher than the values observed for liquid lithiumion electrolytes, typically less than 0.4, and support our assertion

that the current carried by MIT-20-LiCl is dominated by Li⁺ transport.

One approach to changing the polarity of the pore and potentially increasing the conductivity is the installation of softer, less electronegative anions that interact more weakly with the mobile cations, decreasing the activation energy for transport. Owing to its unique ability to allow for large cation loading, MIT-20 is well suited for this purpose. Indeed, reaction of MIT-20 with LiBr followed by exchange of THF with PC led to the isolation of a material with the formula Li_{0.8}[Cu₂Cl₂Br_{0.8}BTDD]·10(PC) (MIT-20-LiBr). Remarkably, even though the molar Li⁺ content of this material is 20% lower than that of MIT-20-LiCl, its conductivity of 4.4×10^{-5} S/cm, determined by ac impedance spectroscopy, is higher, and exceeds the values reported for other MOF-based single-ion Li-ion conductors (i.e. in the absence of added Li⁺ electrolyte).

To ascertain the influence of the pore environment and cation identity on conductivity, we determined the activation energy for ion transport by collecting variable-temperature ac impedance data at 5 °C intervals between 25 °C and 70 °C (Figure S14). In each case, pellets were subjected to a heating-cooling-heating routine (i.e. initial heating to 70 °C, followed by cooling to 25 °C, and re-heating to 70 °C). PXRD analysis after these measurements indicated no significant loss in crystallinity (Figure S15), while infrared spectroscopy showed that all SCN- remained bound within MIT-20-Na (Figure S9). Thus, our materials maintain structural integrity during ion transport measurements. As shown in Figure 3 and Table 1, the activation energy for MIT-20-LiBr, 0.29 eV, is indeed lower than that for MIT-20-LiCl, 0.32 eV, which suggests that further systematic changes in anion identity may improve the ionic conductivity in MIT-20-X, as also shown previously with MOF-74-type materials.^{7b}

Table 1. Ionic conductivity and activation energies for **MIT-20-X** (X = LiCl, LiBr, Na, Mg).

compound	Mo- bile ion	Guest per mole MOF	σ (S/cm)	Ea (eV)	PC per mole of MOF
MIT-20-LiCl	Li^+	1	1.3×10^{-5}	0.32	10
MIT-20-LiBr	Li^+	0.8	4.4×10^{-5}	0.29	10
MIT-20-Na	Na^+	1	1.8×10^{-5}	0.39	9
MIT-20-Mg	$Mg^{2^{+}}$	0.5	8.8×10^{-7}	0.37	8

In summary, the reversible phase transitions from an anionic phase to a neutral one supported by a new copper azolate MOF enable the isolation of stoichiometric amounts of mobile Li⁺, Na⁺, and Mg²⁺ ions in one-dimensional mesopores. The respective Li-, Na-, and Mg-loaded materials function as single-ion solid electrolytes, with conductivity values that are among the highest for these types of electrolytes and activation energies that depend on the nature of the immobile anions. The strategy reported here is enabled by the thermodynamic stability of the anionic MOF phase, its formation presenting a strong driving force for the immobilization of large molar amounts of free ions. Identification of other anionic MOFs that become neutral upon loss of stoichiometric salt equivalents may serve as a blueprint for the design of other single-ion electrolytes.

ASSOCIATED CONTENT

Supporting Information

Synthetic details, single crystal and powder X-ray diffraction data, N_2 adsorption isotherms, TGA, NMR and ac impedance spectra. This material is available free of charge via the Internet at http://pubs.acs.org.

AUTHOR INFORMATION

Corresponding Author

*mdinca@mit.edu

Author Contributions

† S.S.P. and Y. T. contributed equally.

Notes

The authors declare no competing financial interests.

ACKNOWLEDGMENT

This work was supported by the National Science Foundation, through the Waterman Award to M.D. (DMR-1645232). S.S.P. is partially supported by a NSF GRFP (Award No. 1122374). M.D. gratefully acknowledges early career support from the Sloan Foundation, the Research Corporation for Science Advancement, and the Dreyfus Foundation. We thank Dr. P. Mueller and Dr. J. Becker for assistance with crystallography, Prof. J. F. Van Humbeck for assistance with the ac impedance experimental setup, Dr. S. Zhang for helpful discussions on dc measurements, and Dr. L. Sun for electrical conductivity measurements.

REFERENCES

- (a) Tarascon, J.-M.; Armand, M. Nature 2001, 414, 359. (b) Xu, K. Chem. Rev. 2004, 104, 4303. (c) Goodenough, J. B.; Kim, Y. Chem. Mater. 2010, 22, 587.
- (a) Meyer, W. H. Adv. Mater. 1998, 10, 439. (b) Croce, F.; Appetecchi, G. B.; Persi, L.; Scrosati, B. Nature 1998, 394, 456. (c) Fergus, J. W. J. Power Sources 2010, 195, 4554. (d) Kamaya, N.; Homma, K.; Yamakawa, Y.; Hirayama, M.; Kanno, R.; Yonemura, M.; Kamiyama, T.; Kato, Y.; Hama, S.; Kawamoto, K.; Mitsui, A. Nat. Mater. 2011, 10, 682.
- (a) Wright, P. V. MRS Bull. 2002, 27, 597. (b) Van Humbeck, J. F.;
 Aubrey, M. L.; Alsbaiee, A.; Ameloot, R.; Coates, G. W.; Dichtel, W. R.; Long, J. R. Chem. Sci. 2015, 6, 5499.
- (a) Doyle, M.; Fuller, T. F.; Newman, J. Electrochim. Acta 1994, 39, 2073.
 (b) Sadoway, D. R.; Huang, B.; Trapa, P. E.; Soo, P. P.; Bannerjee, P.; Mayes, A. M. J. Power Sources 2001, 97, 621.
 (c) Lin, K.-J.; Li, K.; Maranas, J. K. RSC Adv. 2013, 3, 1564.
 (d) Zugmann, S.; Gores, H. J. Transference Numbers of Ions in Electrolytes. In Encyclopedia of Applied Electrochemistry; Kreysa, G., Ota, K., Savinell, R. F., Eds.; Springer New York: New York, NY, 2014; pp 2086-2091.
- (a) Horike, S.; Umeyama, D.; Kitagawa, S. Acc. Chem. Res. 2013, 46, 2376.
 (b) Yoon, M.; Suh, K.; Natarajan, S.; Kim, K. Angew. Chem. Int. Ed. 2013, 52, 2688.
 (c) Yamada, T.; Otsubo, K.; Makiura, R.; Kitagawa, H. Chem. Soc. Rev. 2013, 42, 6655.
 (d) Ramaswamy, P.; Wong, N. E.; Shimizu, G. K. H. Chem. Soc. Rev. 2014, 43, 5913.
- (a) Zhang, A.; Yoshikawa H.; Awaga, K. J. Am. Chem. Soc. 2014, 136, 16112.
 (b) Fujie, K.; Ikeda, R.; Otsubo, K.; Yamada, T.; Kitagawa, H. Chem. Mater. 2015, 27, 7355.
 (c) Aubrey, M. L.; Long, J. R. J. Am. Chem. Soc. 2015, 137, 13594.
 (d) Vazquez-Molina, D. A.; Mohammad-Pour, G. S.; Lee, C.; Logan, M. W.; Duan, X.; Harper, J. K.; Uribe-Romo, F. J. J. Am. Chem. Soc. 2016, 138, 9767.
 (e) Bai, L.; Tu, B.; Qi, Y.; Gao, Q.; Liu, D.; Liu, Z.; Zhao, L.; Li, Q.; Zhao, Y. Chem. Commun. 2016, 52, 3003.
- (a) Wiers, B. M.; Foo, M.-L.; Balsara, N. P.; Long, J. R. J. Am. Chem. Soc. 2011, 133, 14522. (b) Aubrey, M. L.; Ameloot, R.; Wiers, B. M.; Long, J. R. Energy Environ. Sci. 2014, 7, 667.
- Ameloot, R.; Aubrey, M.; Wiers, B. M.; Gómora-Figueroa, A. P.; Patel, S. N.; Balsara, N. P.; Long, J. R. Chem. Eur. J. 2013, 19, 5533.
- Cepeda, J.; Pérez-Yáñez, S.; Beobide, G.; Castillo, O.; Goikolea, E.; Aguesse, F.; Garrido, L.; Luque, A.; Wright, P. A. Chem. Mater. 2016, 28, 2519

- 10. Rieth, A. J.; Tulchinsky, Y.; Dincă, M. J. Am. Chem. Soc. 2016, 138, 9401.
- 11. Tian, J.-L.; Xie, M.-J.; Liu, Z.-Q.; Yan, S.-P.; Liao, D.-Z.; Jiang, Z.-H. J. Coord. Chem. 2015, 58, 833.12. Evans, J.; Vincent, C. A.; Bruce, P. G. Polymer 1987, 28, 2324.

13. (a) Dia, H.; Zawodzinski, T. A. J. Electroanal. Chem. 1998, 459, 111. (b) Mussini, P. R.; Mussini, T.; Sala, B. Phys. Chem. Chem. Phys. 1999, 1, 5685. (c) Zhao, J.; Wang, L.; He, X.; Wan, C.; Jiang, C. J. Electrochem. Soc. 2008, 155, A292. (d) Zugmann, S.; Fleischmann, M.; Amereller, M.; Gschwind, R. M.; Wiemhöfer, H. D.; Gores, H. J. Electrochim. Acta 2011, 56, 3926.

TOC graphic MIT-20d MIT-20-X Ionic conductivity in MIT-20-X